

## **CHARACTERISTICS OF BOW-TIE SLOT ANTENNA WITH TAPERED TUNING STUBS FOR WIDEBAND OPERATION**

**A. A. Eldek, A. Z. Elsherbeni, and C. E. Smith**

Department of Electrical Engineering  
Center of Applied Electromagnetic Systems Research (CAESR)  
The University of Mississippi  
University, MS 38677, USA

**Abstract**—The characteristics of a bow-tie slot antenna with tapered tuning stubs fed by a coplanar waveguide (CPW) are investigated. The effects of the antenna dimensional parameters are studied through simulation results and design procedure is developed and verified for different frequency bands. The antenna shows wideband characteristics for radar and wireless communication applications. Numerical simulations and measurements indicate that 73% bandwidth can be obtained using the developed design procedure.

### **1 Introduction**

### **2 Antenna Geometry and Parametric Study**

### **3 Measurements**

### **4 Radiation Pattern**

### **5 Conclusion**

### **Acknowledgment**

### **References**

## **1. INTRODUCTION**

In applications where size, weight, cost, performance, ease of installation, and aerodynamic profile are constraints, low profile antennas like microstrip and printed slot antennas are required. Printed slot antennas fed by coplanar waveguide (CPW) have several

advantages over microstrip patch antennas. They exhibit wider bandwidth (BW), lower dispersion and lower radiation loss than microstrip antennas, and the CPW also provides an easy means of parallel and series connection with active and passive elements that are required for matching and gain improvement, and with ease of integration with monolithic microwave integrated circuits (MMIC) [1].

Bow-tie slot antennas have the advantage of wide bandwidth. A number of bow-tie slot designs are introduced in [2–7], which demonstrate wide percentage BW that range from 17% to 40%. In this paper, a bow-tie slot antenna with tapered tuning stubs is introduced. The effects of the antenna parameters on the bandwidth and return loss level of this antenna are also investigated. The parametric study of this antenna yields a design procedure and six designs at different operating frequency bands are introduced to verify that procedure. Measurement results are conducted to verify our results. The related simulation and analysis for these antennas are performed using the commercial computer software package, Momentum of Agilent Technologies, Advanced Design System (ADS), which is based on the method of moment (MoM) technique for layered structures. The ADS simulator, Momentum, is used to solve mixed potential integral equations (MPIE) using full wave Green's functions [8]. Verification of the ADS results is further performed by using the finite difference time domain (FDTD) technique.

## 2. ANTENNA GEOMETRY AND PARAMETRIC STUDY

The proposed antenna and its parameters are shown in Fig. 1 through 3D and  $x$ - $y$  plane views, where  $W1$  and  $L1$  represent the outer width and height of the bow-tie slot, respectively,  $W2$  is the width of the stub,  $L2$  and  $L3$  are the outer and inner heights of the metal stub and  $L4$  is the inner slot height. These antennas are built on a substrate of thickness equals to 30 mil with dielectric constant of 3.2. In this study, a CPW feedline with a 2.9 mm line width and a 0.15 mm slot width is used in order to obtain a  $50\ \Omega$  characteristic impedance.

To confirm the results produced by ADS Momentum, an internally developed FDTD code based on [9] was used to simulate a bow-tie slot antenna with  $W1$ ,  $W2$ ,  $L1$ ,  $L2$ ,  $L3$ ,  $L4 = 19, 14.2, 11.36, 1.76, 1.76$  and  $2.72$  mm, respectively. The convolutional perfect matched layer (CPML) [10] is used to truncate the geometry. Figure 2 shows a comparison between the results of ADS Momentum and FDTD simulations, where a good agreement is observed that validates the results of ADS Momentum. The ADS momentum package is used for the analysis as it provides a faster simulation relative to that based on

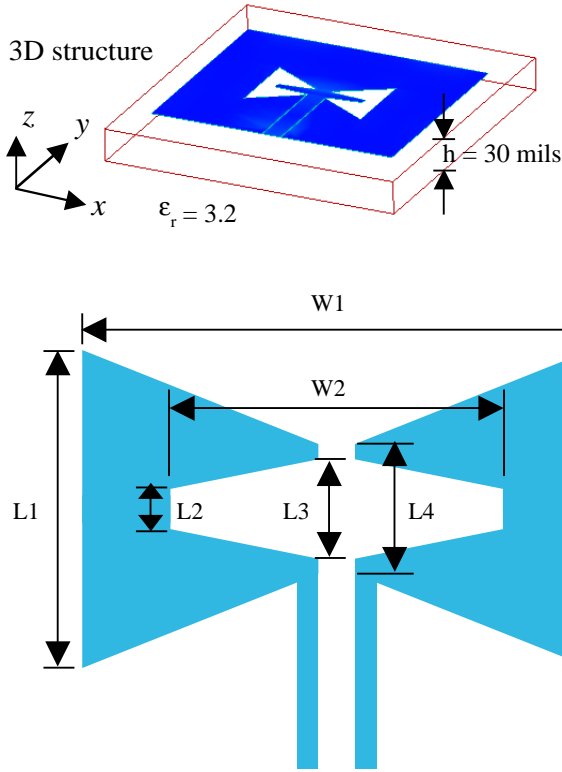


**Figure 1.** The geometry of the proposed antenna.

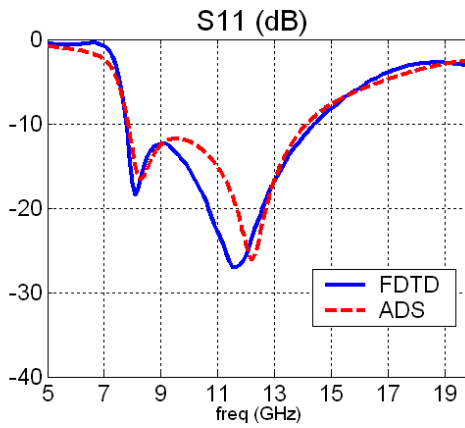


**Figure 2.** FDTD verification of ADS results.

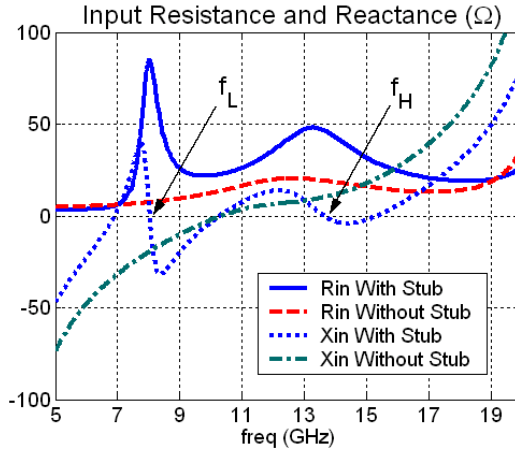


**Figure 3.** The effect of adding the metal stub on the input resistance and reactance.

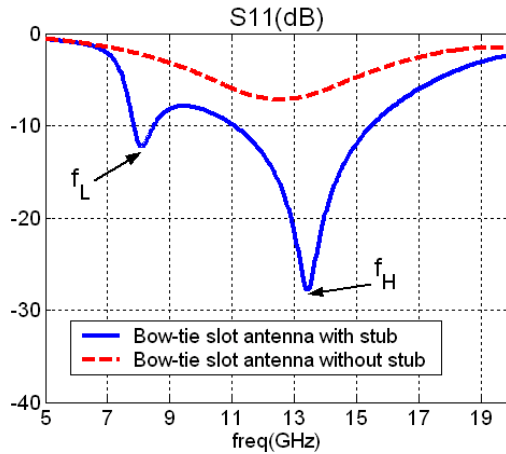


**Figure 4.** The effect of adding the metal stub on the return loss.

the FDTD technique.

The initial design of the proposed geometry has  $W1, W2, L1, L2, L3, L4 = 17, 14.1, 11.62, 0.875, 1.875, 2.68$  mm. In Figs. 3 and 4, the input impedance and the return loss of this design are compared with those of an antenna of the same dimensions but after removing the stub in order to show the effect of adding the metal stub. It can be noticed that adding the stubs increases the input resistance, which

results in better matching. Moreover, it shifts the main resonance to a lower frequency because it increases the total length of the slot, where the magnetic current flows. On the other hand, it creates a new resonance at a higher frequency. Many parameters contribute to these two resonances however, the main contribution seems to be mainly affected by the choice of  $W1$  and  $W2$ . When  $W2$  is not much smaller than  $W1$ , the lower and higher resonant frequencies,  $f_L$  and  $f_H$ , respectively, become close to each other, which gives this design the potentiality of wideband operation. If the return loss levels at the frequencies in-between  $f_L$  and  $f_H$  are less than  $-10$  dB, the antenna will have a wide impedance BW, which can be achieved by a proper selection of the antenna parameters. Thus, the knowledge about the effect of each parameter on the return loss is of great value to get the required design.

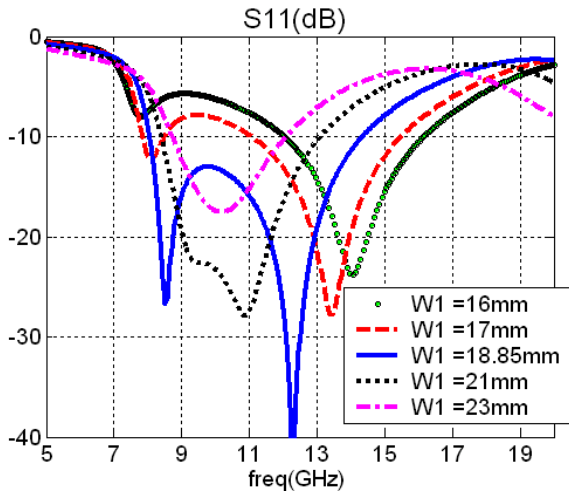


**Figure 5.** The effect of changing  $W1$ .

First,  $W1$  is varied from 16 to 23 mm. It can be noticed from Fig. 5 that decreasing  $W1$  from 23 to 16 mm decreases  $f_L$  and increases  $f_H$ , which results in increasing the difference between the two resonance frequencies and increasing the percentage BW when the return loss level in between is less than  $-10$  dB. When  $W1 = 18.85$  mm the BW = 64%, while it is 47% at  $W1 = 21$  mm and 33% at  $W1 = 23$  mm. It is also noticed that increasing  $W1$  from 16 up to 21 mm improves the return loss level in the range between  $f_L$  and  $f_H$ . Next, the effect of changing  $L1$  is studied corresponding to  $W1 = 18.85$  mm, where the best BW was obtained in the previous simulation. As shown in

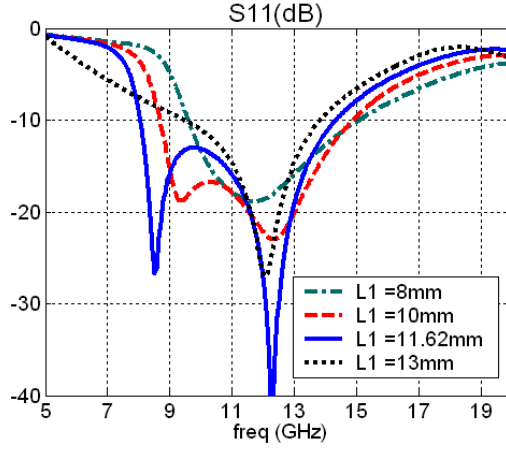


**Figure 6.** The effect of changing  $L1$ .

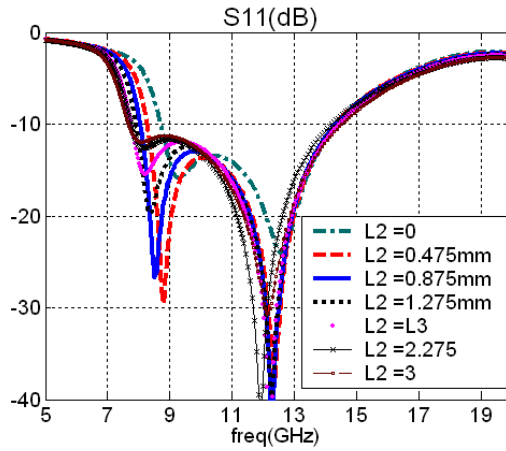


**Figure 7.** The effect of changing  $L2$ .

Fig. 6,  $L1$  controls the return loss level at the two resonances. As  $L1$  increases from 8 to 11.62 mm, both the BW and the return loss level at  $f_H$  improves, however further increments result in reductions in the BW. Figure 7 shows the effect of changing  $L2$  from 0 to a height larger than that of  $L3$ . The parameter  $L2$  does not affect the higher resonance level significantly, but it affects the return loss level of the lower resonance, where the antenna has the best return loss level at  $L2 = 0.475$  mm. Moreover, by increasing  $L2$  the BW increases because

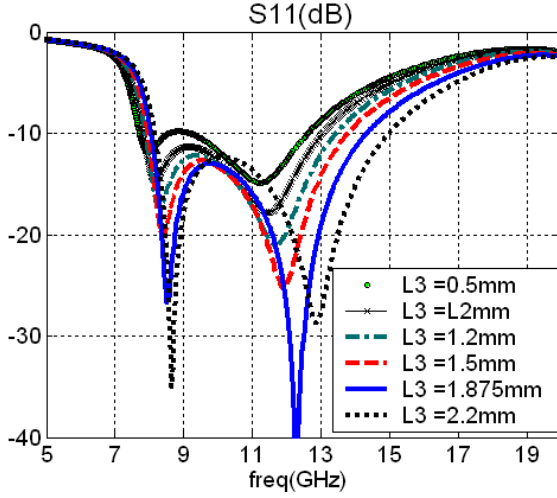


**Figure 8.** The effect of changing  $L3$ .

$f_L$  is shifted to a lower frequency. As shown in Fig. 7, the percentage BW increases from 57% at  $L2 = 0$  to 68% at  $L2 = 3$  mm. Figure 8 presents the effect of changing  $L3$ . Increasing  $L3$  increases the BW because it shifts the higher resonance to a higher frequency. As  $L3$  increases from 0.5 mm to 2.2 mm, the percentage BW increases from 48% to 70%. It also controls the return loss level at  $f_L$ , where its best level is at  $L3 = 2.2$  mm. Further study for this parameter with respect to  $\lambda_H$  shows that  $L3$  should be  $\geq 0.08\lambda_H$  with  $L4$  as an upper limit. Figure 9 shows the effect of changing  $L4$ . Because increasing  $L4$  decreases the flair angle of the bow and decreases the percentage BW. As  $L4$  varies from 2 to 3 mm the BW decreases from 69% to 60%. Increasing  $L4$  also shifts both resonances to lower frequencies, but this change has more effect on the higher resonance. Finally, the effect of changing  $W2$  from 12.1 to 16.1 mm is shown in Fig. 10. As the width of the stub  $W2$  increases, the lower resonance frequency shifts to a lower frequency while the higher one is kept almost at the same position resulting in a wider BW to a certain limit as shown in Fig. 10. As  $W2$  increases from 13.1 to 15.1 mm the percentage BW increases from 60% to 67%.

The values of each parameter are calculated as a function of wavelength at the lower and higher frequencies  $\lambda_L$  and  $\lambda_H$ , where  $\lambda_L = c/f_L$ ,  $\lambda_H = c/f_H$  and  $c$  is the speed of light. Table 1 shows  $W1/\lambda_L$  and  $W1/\lambda_H$  ratios, where it can be concluded that  $W1 \approx 0.77\lambda_H$ . Table 2 shows  $L1/\lambda_L$  and  $L1/\lambda_H$  ratios, where it is

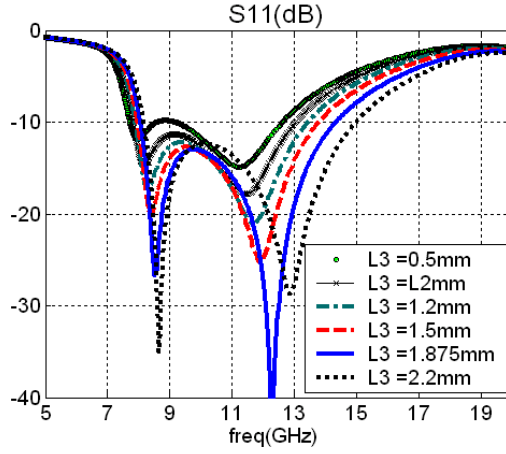


**Figure 9.** The effect of changing  $L4$ .

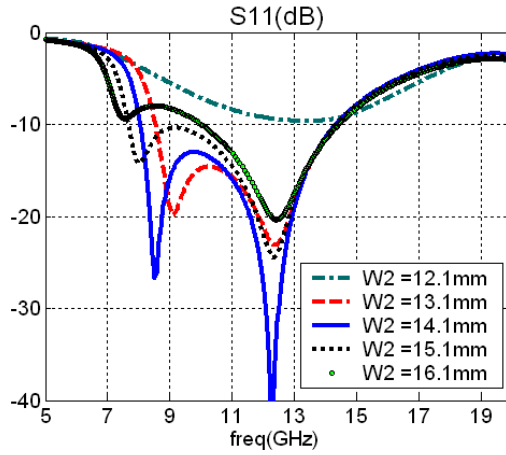


**Figure 10.** The effect of changing  $W2$ .

**Table 1.** Effect of  $W1$  (mm) on  $f_L$  and  $f_H$ .

$W1$ (mm)	16	17	18.85	21	23
$W1/\lambda_L$	0.41	0.45	0.53	0.64	0.77
$W1/\lambda_H$	0.76	0.77	0.77	0.77	0.77



**Table 2.** Effect of  $L1$  (mm) on  $f_L$  and  $f_H$ .

$L1$ (mm)	8	10	11.62	13
$L1/\lambda_L$	0.33	0.33	0.33	—
$L1/\lambda_H$	0.33	0.42	0.48	0.53

**Table 3.** Effect of  $W2$  (mm) on  $f_L$  and  $f_H$ .

$W2$ (mm)	13.1	14.1	15.1	16.1
$W2/\lambda_L$	0.40	0.40	0.40	0.40
$W2/\lambda_H$	0.54	0.58	0.62	0.67

**Table 4.** The design parameters of a bow-tie antenna with a tapered stub with respect to  $\lambda_0$  at  $f_L$  or  $f_H$ , where  $\lambda_L$  and  $\lambda_H$  are  $\lambda_0$  at  $f_L$  and  $f_H$ , respectively.

Parameter	$W1$	$L1$	$L2$
Suggested Initial Value	$0.77\lambda_H$	$0.33\lambda_L$	$0.03\lambda_L$
Parameter	$L3$	$L4$	$W2$
Suggested Initial Value	$0.09\lambda_H$	$0.10\lambda_H$	$0.40\lambda_L$

observed that  $L1 \approx 0.33\lambda_L$ . Table 3 shows  $W2/\lambda_L$  and  $W2/\lambda_H$  ratio, where it can be concluded that  $W2 \approx 0.4\lambda_L$ . The other parameters seem to have upper and lower limits according to the results shown in Figs. 7, 8 and 9. Our study shows that  $L2$  should be  $\leq 0.06\lambda_L$  otherwise the return loss at  $f_L$  will exceed  $-10$  dB,  $L3$  value lies between  $0.08\lambda_H$  and  $L4$ , and  $L4$  value is  $\leq 0.12\lambda_H$ .

The conclusion of this parametric study is given in Tables 4 and 5. In Table 4 we suggest the initial value of  $W1$  to be  $0.77\lambda_H$ ,  $L1$  to be  $0.33\lambda_L$  and  $W2$  to be  $0.4\lambda_L$ . For  $L2$ ,  $L3$  and  $L4$ , we suggested values within their ranges aforementioned. Using this table, an initial guess of the value of each parameter can be assigned when  $f_L$  and  $f_H$  are defined. Table 5 summarizes the effect of increasing each parameter on  $f_L$ ,  $f_H$ , and the BW. Using the data in Table 5, we can improve the results of the initial design.

The outcome of this study became more valuable as it became

**Table 5.** The effects of increasing each parameter on  $f_L$ ,  $f_H$  and BW, where “I” and “D” mean an increase and decrease in the parameter value, respectively.

	$W1$	$L1$	$L2$	$L3$	$L4$	$W2$
$f_L$	I	D	D	—	—	D
$f_H$	D	—	—	—	D	—
BW	D	I	I	I	D	I

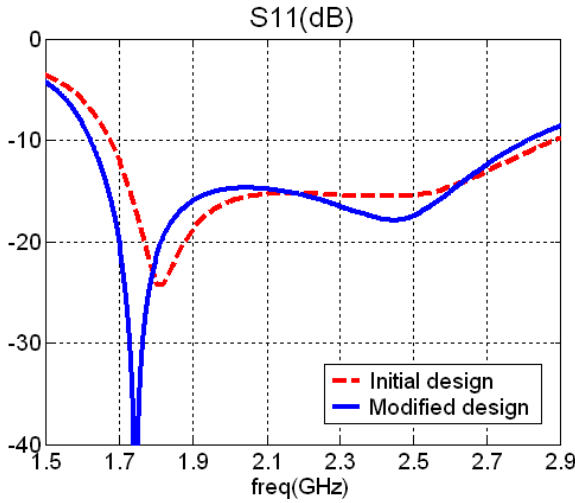


**Figure 11.** Bow-tie slot with stub for 1.75 and 2.45 GHz.

suitable for designing this type of antenna for different frequency bands. As an example, an antenna is designed to operate at 1.75 and 2.45 GHz for personal communications and wireless local area networks (WLAN). For this case,  $f_L = 1.75$  GHz and  $f_H = 2.45$  GHz. Using Table 4 we construct an initial design of  $W1 = 0.77\lambda_L/f_H = 94.286$ ,  $L1 = 0.33\lambda_L = 56.57$ ,  $L2 = 0.03\lambda_L = 5.14$ ,  $L3 = 0.09\lambda_L = 11.02$ ,  $L4 = 0.1\lambda_L = 12.25$  and  $W2 = 0.4\lambda_L = 68.57$  mm, with a CPW of a 3 mm feedline width and a 0.16 mm slot width on a substrate of  $\epsilon_r = 3.2$  and thickness = 30 mils. Using Table 5, slight changes in the initial design is performed to improve the return loss and the BW. The modified design has  $W1$ ,  $W2$ ,  $L1$ ,  $L2$ ,  $L3$ ,  $L4 = 94.25$ , 66.5, 61.4, 5.14, 10.58, 12.25 mm, respectively. Figure 11 shows the return loss of

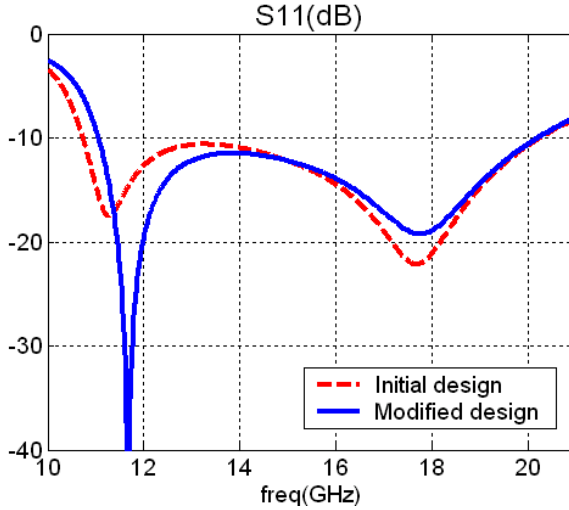


**Figure 12.** Bow-tie slot with stub for Ku band operations.

the initial and modified designs. The initial design is operating from 1.67 to 2.9 GHz, which covers the entire operating frequency band of interest, while the resonances for the modified design are more close to  $f_L$  and  $f_H$ . The modified design has two main resonances at 1.75 and 2.445 GHz, which are approximately the same resonances as specified in the design goals. The antenna is operating from 1.62 to 2.81 GHz with percentage BW = 54% relative to 2.2 GHz center frequency.

To verify the above study in a different frequency band, another antenna is designed for Ku band operation with  $f_L$  and  $f_H$  to be 12 and 18 GHz, respectively, to let the antenna cover the entire Ku band. The initial design using Table 4 suggested that  $W1, W2, L1, L2, L3, L4 = 12.83, 10, 8.25, 0.75, 1.5$  and  $1.67$  mm, respectively and the tuned design makes  $W1, W2, L1, L2, L3, L4 = 13.08, 9.8, 8.25, 0.65, 1.58$  and  $1.67$  mm, respectively, with a CPW of a  $1.53$  mm feedline width and a  $0.1$  mm slot width on a substrate of  $\epsilon_r = 3.2$  and thickness = 30 mils. The return losses of these two designs are shown in Fig. 12. The initial design exhibits wide BW from 10.7 to 21 GHz. The modified design has two main resonances at 11.6 and 17.7 GHz, which are close to the required design values of  $f_L$  and  $f_H$ , with an operating band from 11.1 to 21 GHz and percentage BW = 57.5% relative to 15.5 GHz center frequency. These two examples at two different frequency bands beside the original examples at the X-band validate the design procedure presented here.

Four other antennas are initially designed based on table 4 for Ka

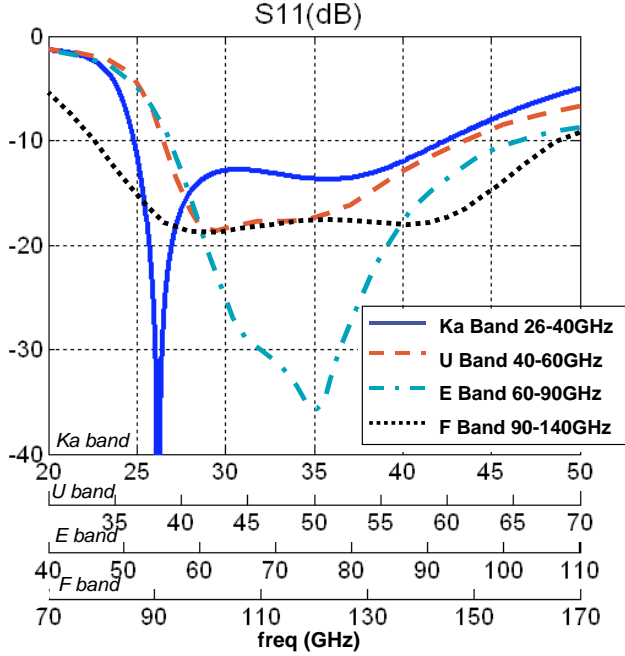


**Figure 13.** Designed antennas for Ka, U, E and F bands.

band, from 26.5 to 40 GHz, U band, from 40 to 60 GHz, E band, from 60 to 90 GHz and F band, from 90 to 140 GHz. Figure 13 shows the return loss of these antennas. The corresponding percentage BW for the antennas for Ka, U, E and F bands are 55%, 48%, 63%, and 73%, respectively.

### 3. MEASUREMENTS

Two antennas of dimensions  $(W1, W2, L1, L2, L3, L4) = (18.85, 14.1, 11.62, 0.875, 2.2, 2.68 \text{ mm})$  and  $(94.25, 66.5, 61.4, 5.14, 10.58, 12.25 \text{ mm})$  proposed for  $X$  and  $R$  frequency bands are fabricated and measured using the HP 8510C vector network analyzer. The fabricated antennas have finite ground plane truncated at 1.8 cm and 5 cm away from the bow-tie slot edge for the  $X$ -band and  $R$ -band antennas, respectively. The return loss of these two antennas is shown in Fig. 14 and 15. As shown in these two figures, there is a very good agreement between the measurements and simulation results. The difference between the measured and the computed return loss is a result of the physical difference between the fabricated and simulated antennas, as

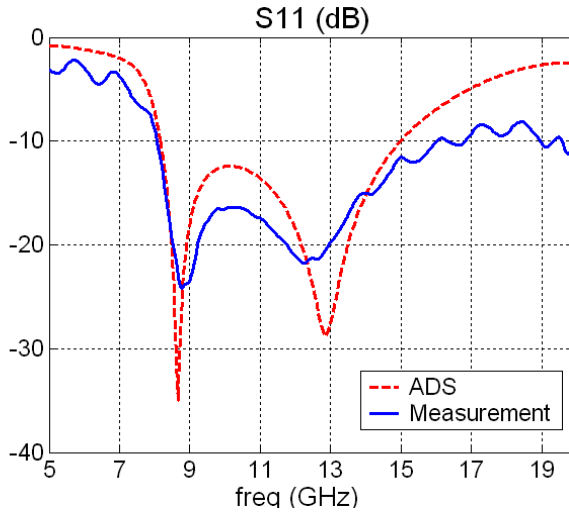


**Figure 14.** Return loss for antenna designed at the X-band.

ADS Momentum package assumes an infinite substrate even with finite ground plane, which is not the case with the fabricated antennas. The antenna at the X-band is operating from 8 GHz to 16.8 GHz, achieving 73% bandwidth, while the second antenna is operating from 1.61 GHz to 3.04 GHz with a 66.5% bandwidth.

#### 4. RADIATION PATTERN

Figures 16 to 17 show the radiation patterns for the  $H$ - and  $E$ -planes, respectively, for the antenna designed for X band. The patterns are computed at 9 GHz, 10 GHz, and 11 GHz to show the stability of the radiation pattern across the band. The antenna has high cross polarization level in the  $H$ -plane due to the contribution of the magnetic current in  $y$ -direction. The radiation pattern for the  $R$ -band antenna is similar to that of the X-band but with slight difference in the cross polarization level. The gain of the X band antenna is computed using ADS with finite ground plane supporting the aperture antenna in order to simulate the fabricated model. The antenna gain within thin X-band is found to range from approximately 5.8 dB to 6.8 dB as shown in Fig. 18.

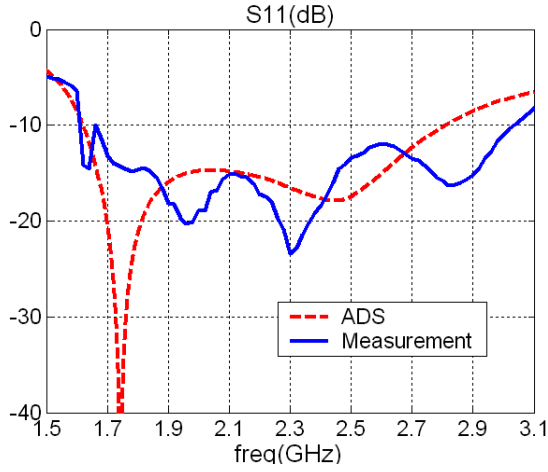


**Figure 15.** Return loss for antenna designed at the  $R$ -band.

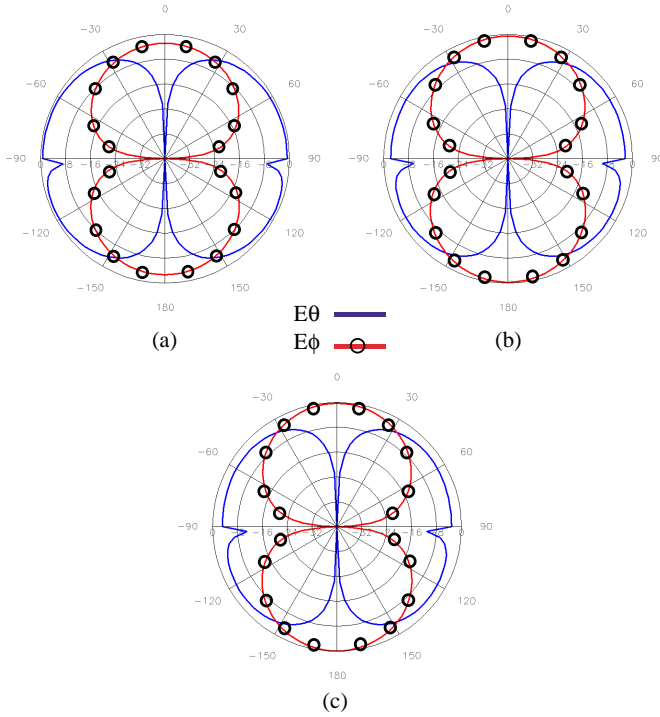


**Figure 16.** Far field pattern in  $H$ -plane ( $x$ - $z$ ) at (a) 9 GHz, (b) 10 GHz, and (c) 11 GHz.

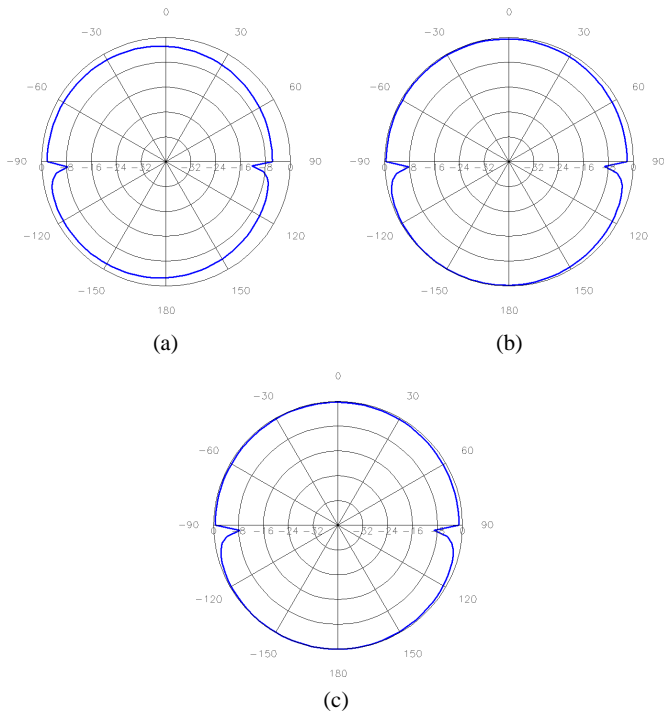


**Figure 17.**  $E_\theta$  pattern in  $E$ -plane ( $y$ - $z$ ) at (a) 9 GHz, (b) 10 GHz, and (c) 11 GHz.

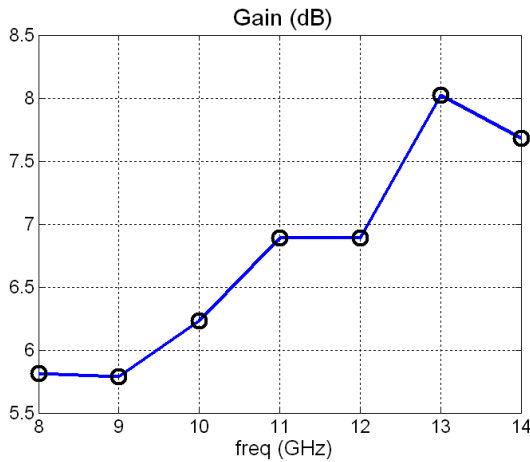


**Figure 18.** Computed gain for the X-band antenna with finite ground plane truncated at 1.8 cm from the antenna edge.

## 5. CONCLUSION

The characteristics of a bow-tie slot antenna with tapered symmetrical tuning stubs are presented. Design procedure has been devised and used to design antennas for different frequency bands of operation. The Bandwidth of the antenna ranges from 48% to 73%. The antenna has high cross polarization level in the  $H$ -plane, however this is acceptable for certain wireless applications. The measurement results confirmed the validity of the antenna for wideband operation.

## ACKNOWLEDGMENT

The authors would like to thank Mr. Aikmin Choong for fabricating the antennas presented in this paper.

## REFERENCES

1. Simons, R. N., *Coplanar Waveguide Circuits, Components, and Systems*, 1–6, 422–424, John Wiley & Sons, Inc., New York, 2001.
2. Lin, Y. D. and S.-N. Tsai, “Coplanar waveguide-fed uniplanar bow-tie antenna,” *IEEE Trans. Ant. Prop.*, Vol. AP-45, No. 2, 305–306, Feb. 1997.
3. Eldek, A. A., A. Z. Elsherbeni, C. E. Smith, and K-F Lee, “Wideband slot antennas for radar applications,” *Proc. IEEE Radar Conf.*, 79–84, Huntsville, AL, May 2003.
4. Soliman, E. A., S. Berbels, P. Delmotte, G. A. E. Vandenbosch, and E. Beyne, “Bow-tie slot antenna fed by CPW,” *Electron Lett.*, Vol. 35, 514–515, 1999.
5. Huang, J. F. and C.-W. Kuo, “CPW-fed bow-tie slot antenna,” *Microwave Opt. Technol. Lett.*, Vol. 19, No. 5, 358–360, Dec. 1998.
6. Miao, M., B. L. Ooi, and P. S. Kooi, “Broadband CPW-fed wide slot antenna,” *Microwave Opt. Technol. Lett.*, Vol. 25, No. 3, 206–211, May 2000.
7. Eldek, A. A., A. Z. Elsherbeni, and C. E. Smith, “Wideband bow-tie slot antennas for radar applications,” *2003 IEEE Topical Conference on Wireless Communication Technology*, Honolulu, Hawaii, October 2003.
8. Agilent Technologies, *Advance Design Systems 1.5 Momentum*, Appendix A, December 2000.
9. Elsherbeni, A. Z. and A. W. Glisson, “The finite difference time domain for electromagnetic applications,” *The Applied*



*Computational Electromagnetic Society (ACES) Conference*, Monterey, March 2003.

10. Roden, J. A. and S. D. Gedney, "Convolutional PML (CPML): an efficient FDTD implementation of the CFS-PML for arbitrary media," *Microwave Opt. Tech. Lett.*, Vol. 27, No. 5, 334–339, 2000.

**Abdelnasser A. Eldek** received an honor B.Sc. degree in Electronics and Communications Engineering from Zagazig University, Zagazig, Egypt, in 1993 and an M.S. degree in Electrical Engineering from Eindhoven University of Technology, Eindhoven, The Netherlands, in 1999. He was a research assistant with the Electronic Research Institute, in Cairo, Egypt, from 1995 to 1997, and from 1997 to 1999 he was a Master student at Eindhoven University of Technology. From 1999 to 2000 he was assistant teacher in the Industrial Education College, Beni Suif, Egypt. He is currently working towards his Ph.D. degree and is a research assistant at the Department of Electrical Engineering, the University of Mississippi.

**Atef Z. Elsherbeni** received an honor B.Sc. degree in Electronics and Communications, an honor B.Sc. degree in Applied Physics, and a M.Eng. degree in Electrical Engineering, all from Cairo University, Cairo, Egypt, in 1976, 1979, and 1982, respectively, and a Ph.D. degree in Electrical Engineering from Manitoba University, Winnipeg, Manitoba, Canada, in 1987. He joined the faculty at the University of Mississippi in August 1987 as an Assistant Professor and advanced to the rank of Associate Professor on July 1991, and to the rank of Professor on July 1997. Dr. Elsherbeni has published 73 technical journal articles and 12 book chapters on applied electromagnetics, antenna design, and microwave subjects, and contributed to 210 professional presentations. He is the coauthor of the book entitled *MATLAB Simulations for Radar Systems Design*, CRC Press, 2003. Dr. Elsherbeni is a senior member of the Institute of Electrical and Electronics Engineers (IEEE).

**Charles E. Smith** was born in Clayton, AL, on June 8, 1934. He received the B.E.E., M.S., and Ph.D. degrees from Auburn University, Auburn, AL, in 1959, 1963, and 1968, respectively. In late 1968, he accepted the position of Assistant Professor of Electrical Engineering with The University of Mississippi, University, MS, and he advanced to the rank of Associate Professor in 1969. He was appointed Chairman of the Department of Electrical Engineering in 1975, and he is currently Professor and Chair of this department.